(12)

AD A112583

DIAGNOSTICS DEVELOPMENT FOR E-BEAM EXCITED AIR CHANNELS

Semiannual Technical Report No. 1

ABSORPTIONS IN E-BEAM EXCITED AIR

February 18, 1982

By: D. J. Eckstrom and J. S. Dickenson

Sponsored by:

DEFENSE ADVANCED RESEARCH PROJECTS AGENCY
1400 Wilson Blvd.
Arlington, VA 22209

Monitored by:

OFFICE OF NAVAL RESEARCH
800 North Quincy Street
Arlington, VA 22217

ARPA Oder No. 4128
Contract No. N000014-81-C-0208
Effective Date: 15 January 1981
Expiration Date: 14 April 1981
Principal Investigator: D. J. Eckstrom (415) 859-4398

SRI Project PYU 2690
MP Report No. 82-119

SRI International
333 Ravenswood Avenue
Menlo Park, California 94025
(415) 326-6200
TWX: 910-373-2046
Telex: 334 486

SRI International

DIAGNOSTICS DEVELOPMENT FOR E-BEAM EXCITED AIR CHANNELS

Semiannual Technical Report No. 1

ABSORPTIONS IN E-BEAM EXCITED AIR

February 18, 1982

By: D. J. Eckstrom and J. S. Dickenson

Sponsored by:

DEFENSE ADVANCED RESEARCH PROJECTS AGENCY
1400 Wilson Blvd.
Arlington, VA 22209

Monitored by:

OFFICE OF NAVAL RESEARCH
800 North Quincy Street
Arlington, VA 22217

ARPA Oder No. 4128
Contract No. N000014-81-C-0208
Effective Date: 15 January 1981
Expiration Date: 14 April 1981
Principal Investigator: D. J. Eckstrom (415) 859-4398

SRI Project PYU 2690
MP Report No. 82-119

Approved by:

D. C. Lorents, Director
Molecular Physics Laboratory

SRI International®

CONTENTS

ILLUSTRATIONS

SUMMARY

The objective of this research program is to develop diagnostics for e-beam excited air channels; these diagnostics are intended to aid the study of propagation of high energy electron beams in air. Our primary task during this first year has been to develop and calibrate an optical system for determination of vibrational and rotational temperatures in the air channel during the e-beam pulse. Secondary tasks involve emission spectroscopy studies to search for an improved optical Faraday cup for primary beam current and for a way to measure temperature in the air channel following the pulse.

In addition to the above tasks, we have recently carried out and report here an experimental determination of absorption in e-beam excited air channels. Measurements were made at 9 Ar^+ laser wavelengths and 5 Kr^+ laser wavelengths, for a low current (4 A/cm^2), long pulse (400 ns) e-beam pump, and for a high current (3000 A/cm^2), short pulse (2.5 ns) e-beam pump. The average absorption coefficient in the low current tests was $\alpha \sim 3 \times 10^{-4}$/cm, and in the high current tests it was $\alpha \sim 3 \times 10^{-3}$/cm. In the short pulse tests, the absorption peaked ~ 3 ns after the fluorescence (on average) and decayed with approximately a 10 ns rate. The strengths, the time histories, and the current dependences of the absorptions suggest that the absorbing species is a positive ion.

Based on these results, we expect that the steady state absorption at visible wavelengths for high current e-beams like the Experimental Test Accelerator and the Advanced Test Accelerator at Lawrence Livermore National

Laboratory will be $\alpha \simeq 3 \times 10^{-2}$/cm. The absorption will increase exponentially with $\sim$ 10 ns time constant. Then, the absorption at t = 1 ns for a step front current pulse will be $\alpha \sim 3 \times 10^{-3}$/cm.

I INTRODUCTION

As the tempo of development of particle beam weapons increases, more detailed diagnostics of the interaction of the particle beam with the atmosphere are being proposed and implemented. Some of these diagnostics involve probing of the excited air channel with visible wavelength laser radiation. Examples include the use of visible wavelength interferometry to measure electron density profiles in the nose of the beam [Ri81] and Stark shift measurements to determine self-induced electric fields [Hi81,DR81]. In these diagnostics, the change in laser intensity due to the desired diagnostic effect can be quite small, leading to the possibility that other effects, such as gas phase absorption, could seriously interfere with the measurement. It is well known that electron-beam pumped laser media always exhibit visible wavelength absorptions during the e-beam pulse. In some cases, the absorption can be identified with a specific atomic or molecular transition, but this is not always possible. In particular, the pure rare gases excited by an e-beam exhibit a continuous background absorption that has not yet been assigned [ZHN79].

We have conducted an experimental program to determine the magnitude of visible wavelength absorption (specifically, on Ar^+ and Kr^+ laser lines) in air excited by an electron beam. The measurements consisted of two phases. In the first phase, a low-current, long-path excitation source was used. When the results of those tests indicated the possibility that high-current beams would cause large absorption, the measurements were repeated using a short-path, high-current source. The results of both phases are reported here.

II EXPERIMENTAL DETAILS

Electron-Beam Sources

The first set of experiments were performed using a Maxwell Excitron e-beam source, which provided a 400-ns pulse of 350-kV electrons with a current density of 4 A/cm^2 over a 50-cm path. The e-beam was fitted with a cell that was filled to 1 atm with laboratory air. The beam is quite uniform both spatially and temporally during the pulse, and steady-state conditions exist during all but the initial rising portion of the pulse. The current-pathlength product was ~ 200 A/cm.

In the second set of experiments, the excitation was provided by a Febetron 706, which produces a 2.5-ns FWHM pulse of 600-kV electrons. A Faraday cup with a 0.6-mm-diameter aperture was used to measure the spatial and temporal e-beam profile. The results of a scan across the beam centerline are shown in Figure 1. The peak current was ~ 2200 A/cm^2, and the FWHM was 1.2-cm. The total current was ~ 4300 A, and the integrated current path length experienced by a probe laser beam was $\int j_b dx \approx 3000$ A/cm. No cell was used; the e-beam traversed laboratory air for 9.5-cm, then it impinged on a plate that was symmetrically grounded back to the e-beam case. The temporal history of the e-beam pulse is shown in Figure 2; the pulse is nearly triangular with ~ 2.5-ns FWHM.

Optical System

In both sets of experiments, we used a Spectra Physics Model 171-17 argon ion laser, prism-tuned to operate on nine different lines, and a Spectra

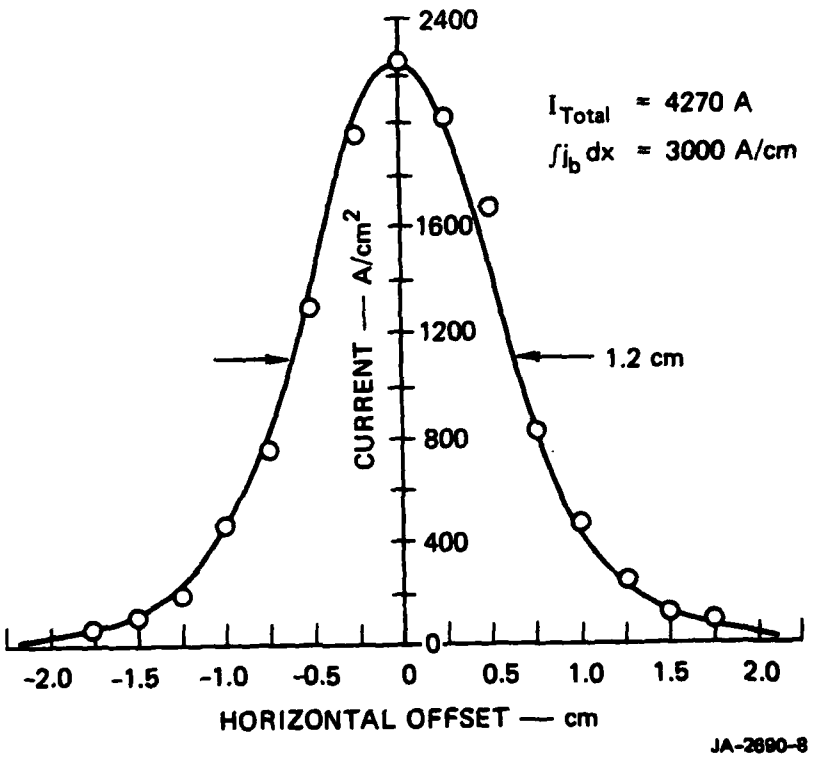

FIGURE 1 RADIAL PROFILE OF CURRENT DENSITY FROM FEBETRON 706 AT PEAK OF PULSE

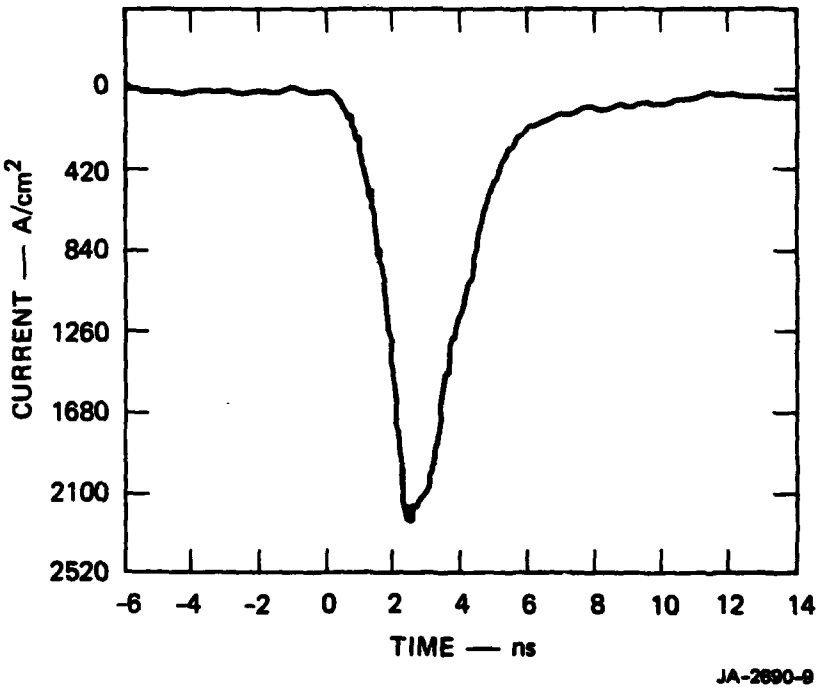

FIGURE 2 TEMPORAL PROFILE OF CENTERLINE CURRENT PULSE FROM FEBETRON 706

Physics Model 171-01 krypton ion laser tuned to five different lines. Neither laser was fitted with an etalon and so operated on several longitudinal modes. This resulted in laser amplitude modulations at approximately 100 MHz; the fluctuations were about $7 \pm 3\%$ of the average intensity. These fluctuations averaged out in the long-pulse measurements, but limited the sensitivity in the Febetron tests.

In addition, we used a Coherent Radiation Model CR3000K krypton ion laser for measurements on the Febetron. The stability of this laser was worse; the amplitude modulations without an intracavity etalon were about 30%, whereas the etalon reduced the fluctuations to $\sim 1.6\%$. However, the etalon also caused a substantial reduction in output power.

The laser was mechanically chopped to provide a 1-ms pulse at 1% duty cycle, which prevented saturation of the detector. A beam splitter reflected a fraction of the pulse into a photodiode that triggered a time delay generator. After suitable delay, the generator triggered the e-beam source to provide an excitation pulse approximately midway into the chopped laser pulse.

In the first set of experiments, the laser probe beam was passed through the long-path cell, then directed into a screen room where it impinged on a detection photodiode. The total path from the center of the cell to the detector was ~ 4 m. The layout for the Febetron experiments is shown in Figure 3. The laser was focused with a 100-cm focal-length lens on the center of the e-beam, and then refocused with a telescope onto a photodiode that was 3 or 7 meters from the e-beam, depending on the detector. This minimized refraction effects, such as beam steering and/or focusing/unfocusing, that might have been introduced by the beam. A diverging lens or a ground glass plate was placed immediately in front of the photodiode to minimize local saturation effects and to average out spatial nonuniformities in the laser

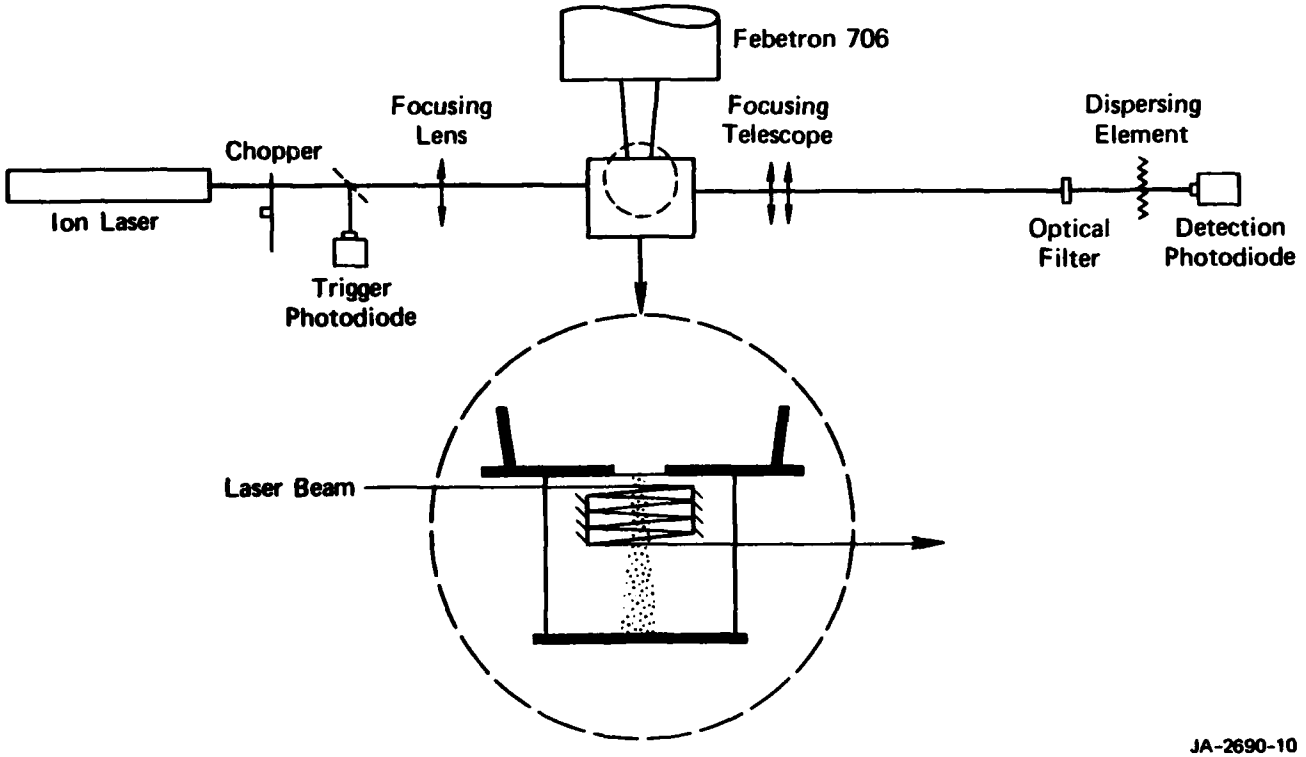

FIGURE 3 SCHEMATIC LAYOUT OF AIR ABSORPTION MEASUREMENTS USING FEBETRON 706

beam. The latter property further reduced any beam steering and focusing effects that might not have been eliminated by the focusing telescope. A filter (usually 10-nm FWHM) that transmitted the laser probe was also placed in front of the photodiode to reduce the airglow fluorescence signal that is produced simultaneously with the excitation pulse.

In the Febetron experiments, the laser probe was multiply passed through the e-beam channel. The mirrors were 5-cm apart and 2.5-cm in diameter, and in all but one set of data reported here, nine passes were used. Since the total light transit time through the mirror system was ~ 1.5 ns, which is on the same order as the e-beam pulse width, the instantaneous absorption measured was a time average over 1.5 ns. However, a careful deconvolution of a typical absorption history gave approximately the same result as neglecting the transit time averaging; therefore all results reported here were calculated simply by dividing the peak instantaneous absorption by the number of passes.

The Maxwell Excitron long path experiments and the first set of Febetron experiments were performed using an ITT Type F4000 vacuum photodiode with S-20 photocathode. The signals from this large area photodiode (4-cm diameter) were very low in some cases, thus limiting the sensitivity of the experiments. In a second set of Febetron experiments, we used an RCA C30817 silicon avalanche photodiode of ~ 1 mm^2 sensitive area and with a sensitivity of ~ 30 A/W in the visible. It was necessary to attenuate the laser beam at all wavelengths to keep from overloading this detector. Although the quoted rise time for the detector is $\tau_r < 2$ ns, we found that it tracked our fluorescence pulses without distortion.

Data Processing

In the long-path, low-current experiments, the photodiode signals were recorded on a Tektronix Type 555 oscilloscope. The 50-MHz bandwidth of this scope averaged out the higher frequency amplitude fluctuations of the laser, while the 400-ns e-beam pulse width made visual signal averaging of the absorption histories straightforward. There was a small residual fluorescence signal in these experiments, which was subtracted out of the data traces before calculating the absorption. The sensitivity in these experiments varied from 0.1 to 1%, depending on the strength of the laser line, while the absorptions observed varied from 1 to 3% (for the total 50-cm path).

In the Febetron experiments, the output of the photodiode was displayed on a Teketronix 7844 oscilloscope, which was used to monitor the chopped beam and set the initial laser intensity. Simultaneously, the signal was fed to a Hewlett Packard Model 8447A amplifier (measured gain 6X), with the amplified signal fed to a Tektronix R7912 transient digitizer. This system was used to record and average 10 consecutive shots conducted under identical conditions (~ 10 shots per minute). In a typical data sequence, the laser was then blocked upstream of the e-beam, and 10 background shots (which included any residual air fluorescence) were recorded and averaged. The final absorption history was the difference between the two averages.

A separate shot was taken with the laser blocked and the optical filter removed to measure the air fluorescence. The fluorescence was assumed to be synchronous with the current pulse, and the relative time histories of the fluorescence and absorption were taken as representing the correlation between the current and absorption histories. Separate shots were also taken to establish the amplitude fluctuations in the laser intensity, both with and without amplification, as reported for the different lasers above.

Efforts were made to eliminate spurious causes for the observed absorptions. We have already noted our use of a focusing telescope and diffusers to minimize refraction effects. We also blocked the e-beam between the source and the laser probe path and verified that rf noise effects were not changing the laser beam intensity. In one case, we rerouted the laser around the unblocked e-beam and verified that there was again no change in laser intensity. Finally, we used four mirrors spaced 2.5 cm away from the e-beam axis and used eight mirror bounces of the laser beam (without traversing the excited air volume) to see whether scattered electrons impinging on the mirrors could cause a momentary reduction in reflectivity that could be mistaken for gas absorption. (In the absorption experiments, the laser experienced eight bounces off two mirrors spaced 2.5 cm from the beam axis.) Again, there was no change in laser intensity observed during the e-beam pulse due to this effect.

Another parameter that can be used to determine if the observed signal was really due to gas phase absorption is the gas composition and/or pressure. Since we were not using a cell, we could not readily change the gas. However, the experimental volume was enclosed in a lead box intended for x-ray and rf attenuation, and we did two experiments at $\lambda = 488$ nm in which we flushed the box thoroughly with N_2 or Ar. The absorptions in both experiments were much stronger than in air ($\alpha = 1.2 \times 10^{-2}$/pass for N_2 and $\alpha = 2.4 \times 10^{-2}$/pass for Ar, compared with $\alpha = 5 \times 10^{-3}$/pass for air), indicating that the absorption is indeed gas phase. The time histories of the N_2 and Ar absorptions were quite similar to those for air.

III RESULTS

Long-Path, Low-Current Experiments

The most definitive data set from this series of tests is shown in Figure 4. The top trace is the e-beam voltage monitor, showing the 400-ns voltage pulse. The middle trace is the laser transmission history, showing absorption during the e-beam pulse. The bottom trace shows the chopped laser signal, which establishes the I_o value. In this case, the total intensity change due to absorption plus fluorescence is 0.74%; subtracting the fluorescence contribution gives an absorption coefficient of 2×10^{-4}/cm. A time correlation between absorption and excitation level cannot be established from this picture because the e-beam current does not turn on and off as rapidly as the voltage.

The absorption coefficients determined for nine Ar^+ laser lines and five Kr^+ lines are shown in Figure 5. With the exception of the result at 454.5 nm, the values are $\alpha = 4 \times 10^{-4}$/cm to within a factor of 2. The error bars shown represent experimental uncertainties (I_o and ΔI) for individual tests.

High-Current Experiments

Initial Febetron experiments conducted in the same way as the long-path experiments showed no evidence of absorption, and it was necessary to make several modifications to the setup to substantially increase the sensitivity. Changes included the addition of mirrors to create a multipass probe of the excited air volume, addition of a signal amplifier, and use of the transient digitizer system to average repetitive signals. Additional efforts were made to reduce the rf noise to levels that did not interfere with

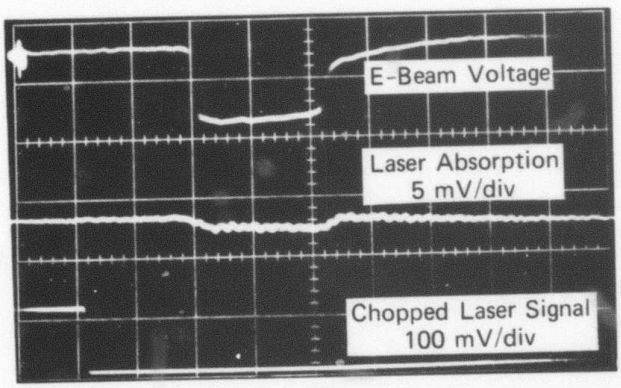

FIGURE 4 ABSORPTION DATA FOR LOW CURRENT, LONG PULSE TEST AT λ = 530.9 nm

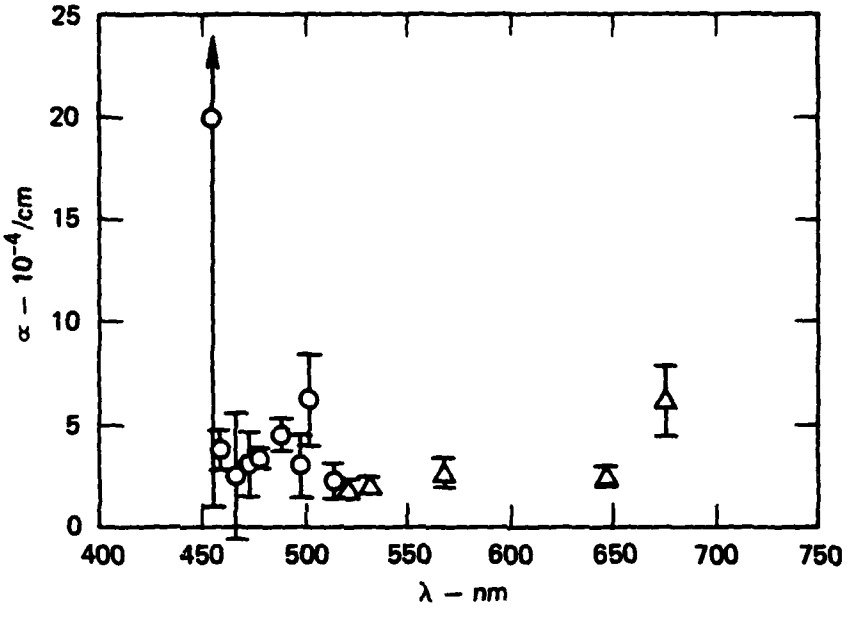

FIGURE 5 ABSORPTION COEFFICIENTS AT Ar^+ AND Kr^+ LASER WAVELENGTHS DETERMINED IN LOW CURRENT, LONG PULSE EXPERIMENTS

(Error bars represent uncertainties in individual measurements.)

the signal. With these modifications, the limitation to the sensitivity was imposed primarily by the fluctuations in the laser intensity. As noted earlier, these averaged about 7% for the Spectra Physics Ar^+ and Kr^+ lasers operated without etalons, and ~ 1.6% for the Kr^+ laser with an etalon. Figure 6(a) shows a single shot transient digitizer recording of an unamplified signal from the Ar^+ laser at 514.5 nm; the highest frequency noise is faster than the system response and so must be spurious fluctuations in the recorder, but an approxiomately 100-MHz fluctuation of ~ 4% peak to peak is clearly seen. A 10-shot average of the same signal shown in Figure 6(b) indicates a smoothing of the ± 4-mV fluctuations to ± 1 mV. However, when the signal is amplified 6 times, Figure 6(c), the randomness of the signal is about ± 8 mV. These traces, taken without firing the e-beam, are representative of the "noise" level of the experiments.

An example of one of the poorer absorption traces (λ = 514.5 nm, signal/noise ≈ 1) is shown in Figure 7(a). One can only be sure that absorption is present by virtue of seeing the same intensity perturbation appear in several repeated shots, with the perturbation correlated with the fluorescence history shown in Figure 7(b). A more convincing absorption history, again at 514.5 nm, but taken with the silicon avalanche photodiode, is shown in Figure 8(a), together with the fluorescence trace in Figure 8(b). These figures illustrate not only a range of signal to noise, but the scatter in the absorption coefficients (1.6×10^{-3}/pass versus 4.5×10^{-3}/pass) and the uncertainty in time delay between peak fluorescence and peak absorption Δt ~ 4 and 1 ns).

A summary of the absorption coefficients determined from these experiments is presented in Figure 9. Points with error brackets are mean values and standard deviations of several shots (the number of shots is given

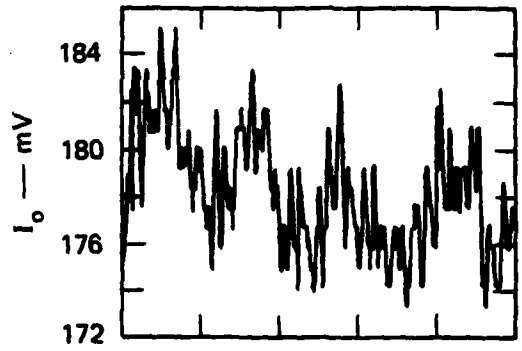

(a) SINGLE SHOT LASER SIGNAL

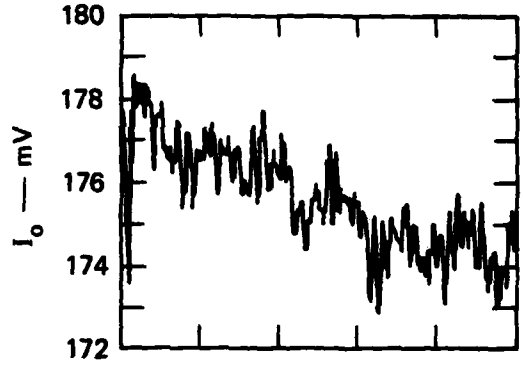

(b) 10 SHOT AVERAGE OF LASER SIGNAL

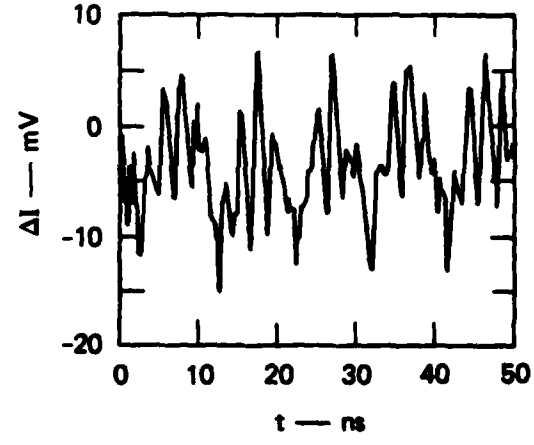

(c) 10 SHOT AVERAGE OF LASER SIGNAL AFTER 6x AMPLIFICATION

JA-2990-13

FIGURE 6 CHARACTERISTIC FAST RESPONSE LASER INTENSITY SIGNALS (λ = 514.4 nm)

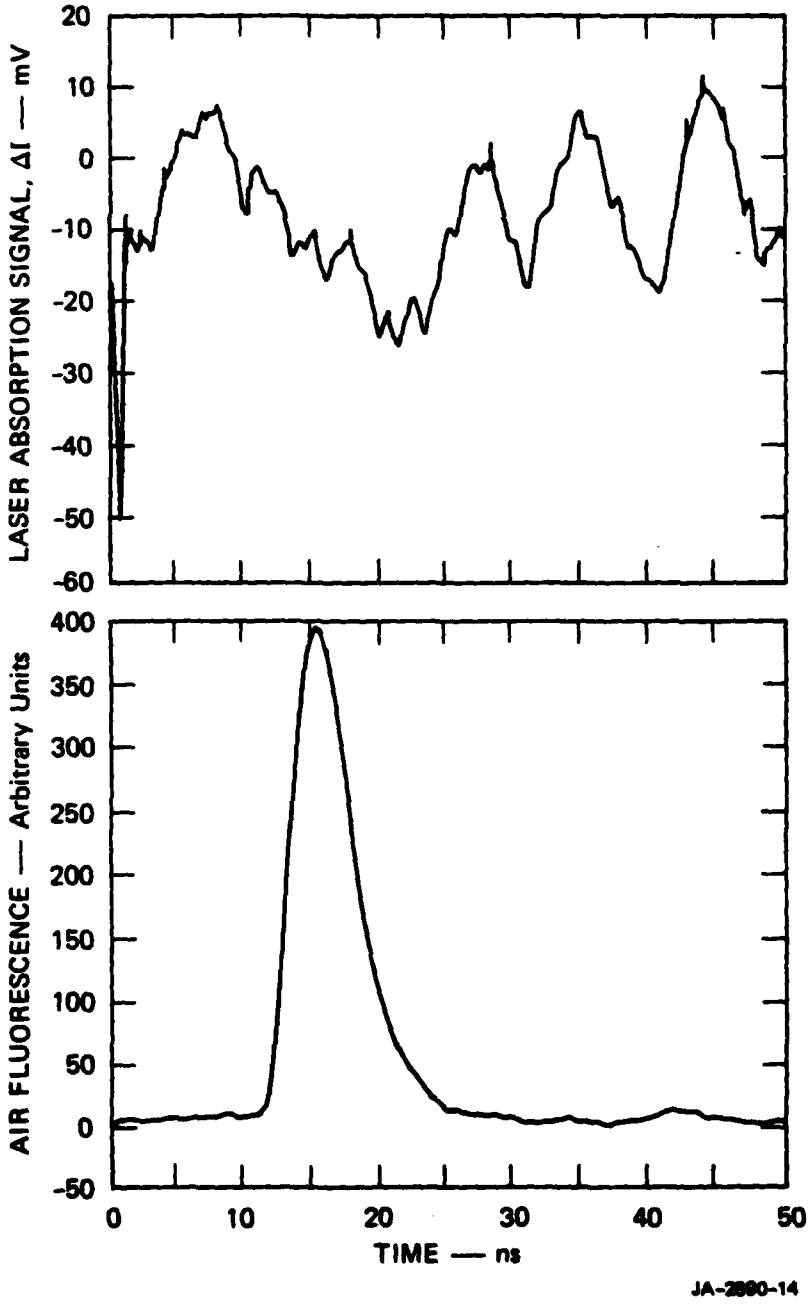

FIGURE 7 LASER ABSORPTION AND FLUORESCENCE SIGNALS AT 514.5 nm FOR HIGH CURRENT, SHORT PULSE EXPERIMENT USING ITT VACUUM PHOTODIODE

(I_o = 1070 mV)

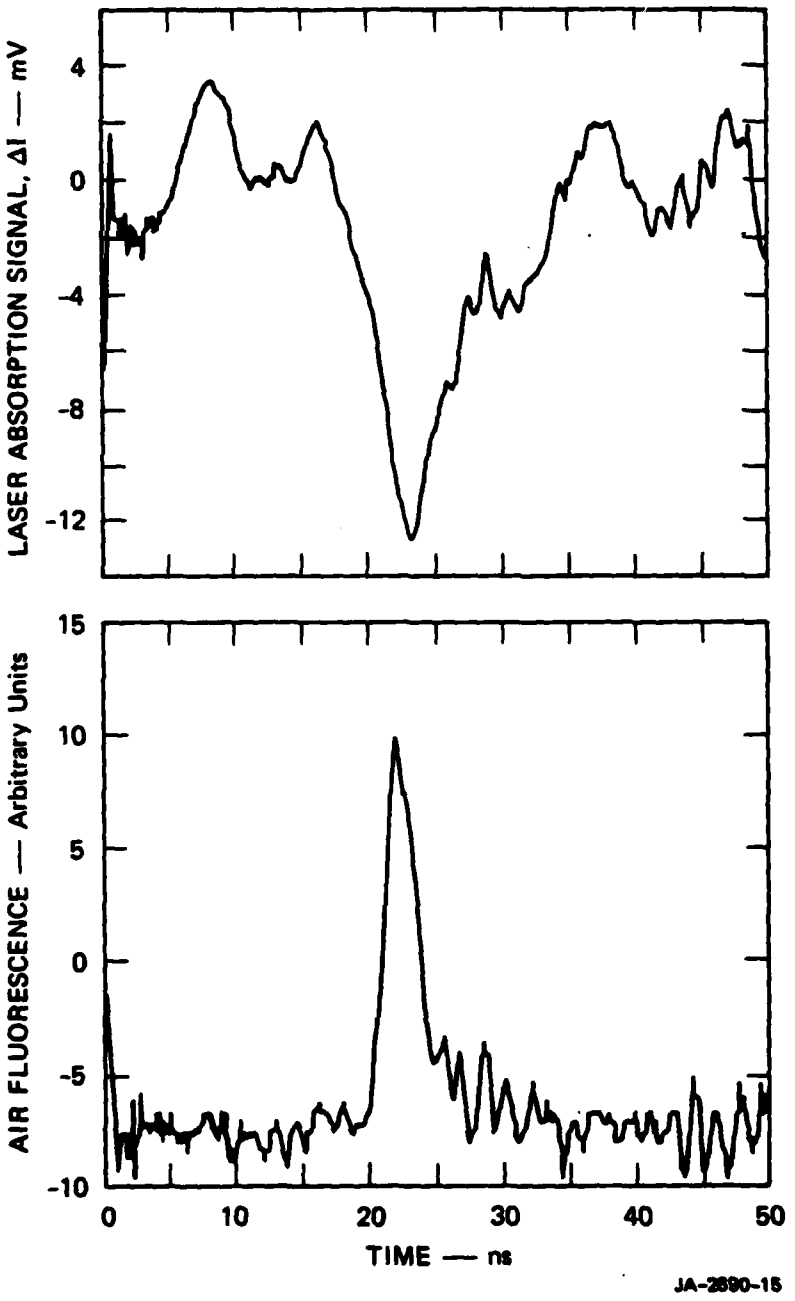

FIGURE 8 LASER ABSORPTION AND FLUORESCENCE SIGNALS AT 514.5 nm FOR HIGH CURRENT, SHORT PULSE EXPERIMENT USING RCA SILICON AVALANCHE PHOTODIODE

(I_o = 300 mV)

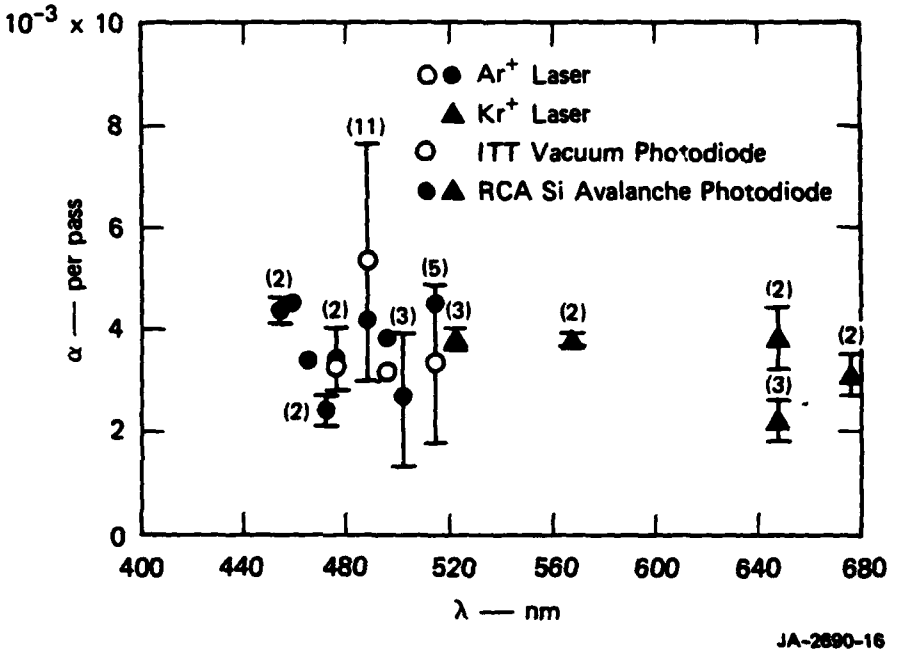

FIGURE 9 ABSORPTION COEFFICIENTS AT Ar^+ AND Kr^+ LASER WAVELENGTHS DETERMINED IN HIGH CURRENT, SHORT PULSE EXPERIMENTS

(Error bars represent standard deviation in number of multiple measurements indicated.)

($\int j_b dx$ = 3000 A/cm^2; 9 pass measurement)

in parenthesis above the bar). Results obtained with the two types of photodiode detectors are presented separately, but are in good agreement with each other. The absorption coefficients vary over the range (2.5-5) x 10^{-3}/pass (1 pass = 1 cm). It is not clear that the absorption has a systematic wavelength dependence, especially since there is little if any correlation between the wavelength dependencies of the low current and high current tests.

The second interesting aspect of the absorption is the time dependence. The absorption is clearly time-correlated with the fluorescence, but quantitative determinations are difficult because of the poor signal-to-noise ratios. The peak of the absorption occurs within a few nanoseconds of the peak of the fluorescence. Mean values and standard deviations of the time delay for the tests at each wavelength are shown in Figure 10. The scatter is large, and one might suspect that larger delays correspond to poorer signal-to-noise (S/N) ratios. However, if the time delay for each test is plotted versus the S/N ratio of that test, as shown in Figure 11, there is no apparent correlation, and we conclude that on the average the absorption peak lags the fluorescence peak by ~ 2.5 ns. The decay of the absorption is also obscured by the random fluctuations in intensity, but examination of all the data suggests an exponential decay with ~ 10-ns time constant.

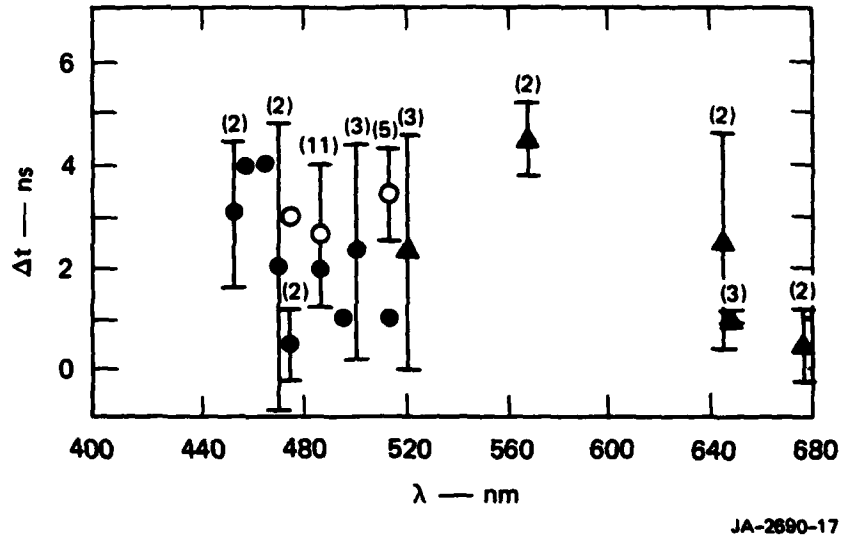

FIGURE 10 TIME DELAY BETWEEN FLUORESCENCE AND ABSORPTION PEAKS IN FEBETRON 706 EXPERIMENTS

(Error bars represent standard deviation in number of measurements indicated.)

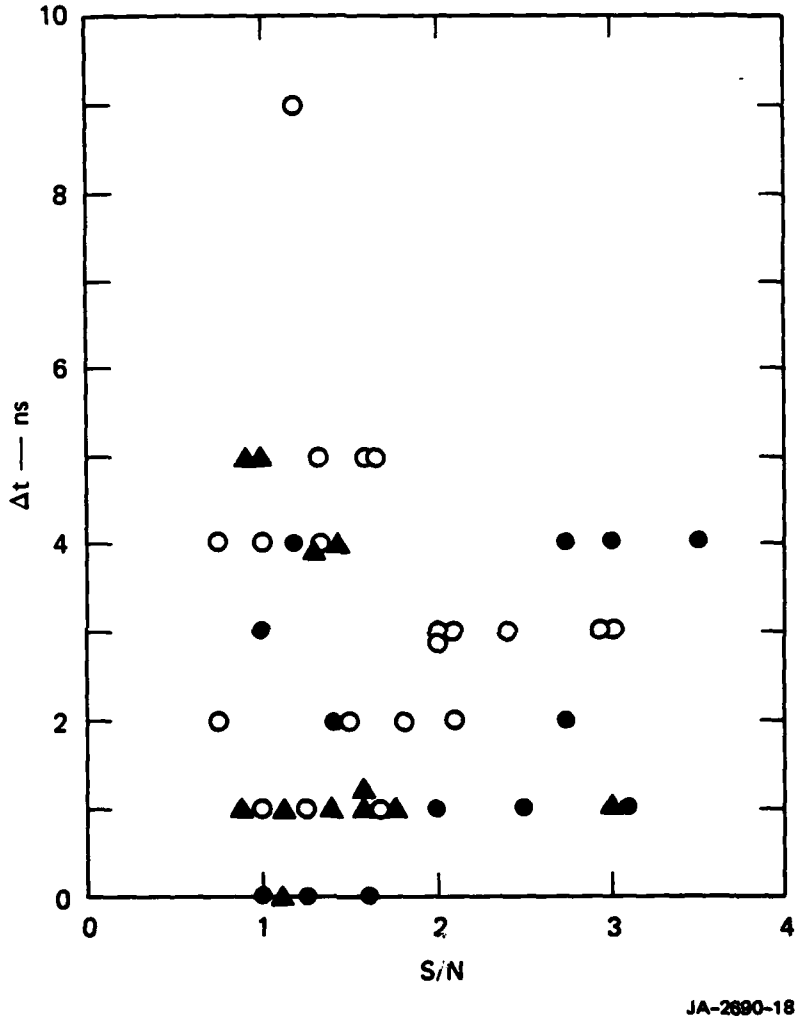

FIGURE 11 CORRELATION OF TIME DELAY BETWEEN FLUORESCENCE AND ABSORPTION PEAKS WITH SIGNAL TO NOISE RATIO

IV DISCUSSION

A major surprise of this study was the weakness of the absorption in the Febetron experiments. The low current tests (4 A/cm^2) showed absorptions of $\sim 4 \times 10^{-4}$/cm. The Febetron produces an equivalent of ~ 3000 A/cm^2, and if absorption were directly proportional to current, it would be ~ 0.3/cm. In fact, it was found to be $\sim 4 \times 10^{-3}$/cm, up by only a factor of 10 rather than 750.

A small part of this nonlinearity with current can be attributed to the fact that the Febetron pulse is too short for steady-state excited state populations of air species to be reached. We noted above that the decay rate for absorption was $\sim$ 10 ns; simple kinetics calculations indicate that the absorbing species might only reach 20% of its steady-state population following a 2-ns Febetron pulse. If we increase the absorption in the Febetron case by a factor of 5 to account for this pulse length effect, the ratio between the high-current and low-current test is still only about 50, compared with the current ratio of 750.

These observations indicate that the absorbing species is probably not a neutral molecular excited state for two reasons. First, excited state populations should be proportional to the excitation rate (i.e., to the current), but the absorption increases less than 1/15 as much as the current. Second, the primary airglow emission that has been observed in the spectral region studied here (540-680 nm) is from the $N_2(B^3\Pi_g \rightarrow A^3\Sigma_u^+)$ "First Positive" system [D064]. Then the N_2 (A) state would be the absorbing species, and the time history of the absorption would reflect the population history of that state. However, N_2 (A) is a long-lived state, with a quenching lifetime in air at 1 atm of 50-70 ns [SWB73;PC81]. The observed absorption decays in about 10 ns, which is much faster than the expected N_2(A) decay.

An argument against assignment of the absorption to $N_2(A)$ can also be made on the basis of the strength of the First Positive transition. The absorption coefficient, α (cm^{-1}), can be expressed approximately as

$$\alpha \simeq \frac{\lambda^3}{8\pi c} \frac{\lambda}{\Delta\lambda} \frac{\Delta N}{\tau}$$

where λ is the wavelength (cm), $\Delta\lambda$ is the spectral width of the absorption (cm), ΔN is the population difference between the lower and upper levels of the transition (cm^{-3}), τ is the transition radiative lifetime (s), and c is the speed of light. We can use the values of $\alpha \simeq 3 \times 10^{-3} cm^{-1}$, $\lambda \simeq 5.5 \times 10^{-5} cm$, $\Delta\lambda \gtrsim 2 \times 10^{-5} cm$, and $\tau \simeq 10^{-5} s$ [Je66] for the First Positive system. We then can calculate that $\Delta N \simeq 5 \times 10^{16}/cm^3$ is required to cause the observed absorption. However, we estimate that the total production of excited states in air by a Febetron pulse is no more than $\sim 3 \times 10^{15}/cm^3$.

The fact that the absorption coefficient increases much less than the current density suggests that the absorbing species population depends on pump rate as P^n, where $n < 1$. An example of such a dependence is the electron and positive ion densities in a regime where the plasma is dominated by recombination. Then the simple rate equation is

$$\frac{dn_e}{dt} = \frac{dN^+}{dt} = P - \alpha n_e N^+$$

and for $n_e = N^+$, the steady-state populations of n_e and N^+ are

$$n_e = N^+ = (P/\alpha)^{1/2}.$$

In this case, $n = 1/2$, and since the pump rate is proportional to current density, these populations would be expected to increase in the Febetron tests over the low-current tests by the ratio $(750)^{1/2} = 27$, which is, in fact, in reasonable agreement with the ratio of absorptions. Unfortunately, over about half of the range of current density, the air plasma is governed not by recombination but by attachment. The rate equation is then

$$\frac{dn_e}{dt} = P - \beta n_e N_a$$

and in steady state the electron density varies as

$$n_e = P/\beta N_a,$$

which is again a linear dependence on j_b. Consideration of both recombination and attachment (using the rates $\alpha = 10^{-7} cm^3/s$ and $\beta N_a = 8 \times 10^7/s$ for 1 atm air) indicates that the steady-state electron density ratio is ~160, compared with a current ratio of ~750.

The positive ion density varies somewhat less than n_e in this simple model, and the negative ion density may vary only slightly with pump rate. The simplified rate model is

$$\frac{dN^+}{dt} = P - \alpha N^+ n_e - \alpha' N^+ N^-$$

$$\frac{dN^-}{dt} = \beta n_e N_a - \alpha' N^+ N^-$$

together with the conservation equation $n_e + N^- = N^+$. Using the somewhat arbitrary rate $\alpha' = 10^{-6}$ cm^3/s gives a ratio between Febetron and Excitron tests for N^+ of ~ 60 and for N^- of ~ 2.6 (compared with a measured absorption ratio of 10 to 50).

This model is so simplified compared with the complex chemistry of air that it can only serve as a guide. However, it does indicate that a positive ion is most likely the absorbing species. There is, of course, still a question of transition strength. The simple model indicates that N^+ populations will be $\simeq 10^{15}$/cm^3. For this population to cause an absorption of 3×10^{-3}/cm requires a radiative lifetime of $\simeq$ 200 ns or a broadband absorption cross section of ~ 3×10^{-18}cm^2. These values are not unreasonable.

In any absorption measurement, one must consider the possibility of free electron inverse bremsstrahlung absorption as the mechanism. In this case, we estimate the electron concentration in the Febetron tests to be less than 3×10^{15}/cm^3. The inverse bremsstrahlung absorption cross section at 550 nm for 1 atm air at an electron temperature of 1 eV is approximately 6×10^{-20} cm^2. Thus, this component of the absorption coefficient is $\alpha \sim 2 \times 10^{-4}$ cm^{-1}, or less than 10% of the observed value.

V CONCLUSIONS

In the experiments reported here, absorptions in e-beam excited air have been found at all wavelengths tested (8-9 Ar^+ laser lines and 4-5 Kr^+ laser lines). The average values of the absorption coefficients were 4×10^{-4}/cm for low-current (4 A/cm^2), long-pulse tests, and 3×10^{-3}/cm for high-current (3000 A/cm^2), short-pulse tests. No wavelength dependence for the absorption can be confidently established. Precautions have been taken to ensure that experimental artifacts were not responsible for the absorption signals. In the short pulse experiments, the absorption peak occurs on average about 3 ns after the air fluorescence peak, and the absorption decays with about a 10-ns time constant.

On the basis of the two current densities studied here, it appears that the absorption scales with current density approximately as $j_b^{1/2}$. Some very simple kinetic modeling suggests that a positive ion species might be the absorber. Known neutral molecular transitions and free electron inverse bremsstrahlung absorptions can probably be ruled out.

The implications of the present results for experiments on the Experimental Test Accelerator at Lawrence Livermore National Laboratory are as follows. We will assume that the steady-state absorption in the Febetron experiments is about 5 times the observed transient value, or about 1.5×10^{-2}/cm. We will also assume that the absorption scales with $j_b^{1/2}$ in the high-current range. Then the steady-state absorption level on ETA will be about 3×10^{-2}/cm. Since the absorption decay time constant was observed here to be $\sim$ 10 ns, the absorption should grow exponentionally with a 10-ns time

constant until the steady-state value is reached. Thus, for a step function current pulse, the absorption after 1 ns should be [1 - exp(-0.1)] of the steady-state value, or about 3 x 10^{-3}/cm.

REFERENCES

DO64 G. Davidson and R. O'Neil, J. Chem. Phys. 41, 3946 (1964).

DR81 N. Djeu and J. Reintjes, "A Proposal for Measuring the Electric Fields in a Charged Particle Beam Propagating in the Atmosphere," Naval Research Laboratory (1981).

Hi81 R. M. Hill, "Stark Effect Measurement of Dynamic Electric Fields," SRI International Molecular Physics Laboratory Research Brief MP81-197R (November 1981).

Je66 M. Jeunehomme, J. Chem. Phys. 45, 1805 (1966).

PC81 L. G. Piper and G. E. Caledonia, J. Chem. Phys. 74, 2888 (1981).

Ri81 Dennis Riley, presentation at the Charged Particle Beam Experimental Coordination Meeting, Lawrence Livermore National Laboratory, 28 October 1981.

SWB73 T. G. Slanger, B. J. Wood, and G. Black, J. Photochemistry 2, 63 (1973/74).

ZHN79 E. Zamir, D. L. Huestis, H. H. Nakano, R. M. Hill, and D. C. Lorents, IEEE J. Quantum Electron. QE-15, 281 (1979).